The Influence of the Equation Type on Iterative Parameter Identification Problems which are Elliptic or Hyperbolic in the Parameter

Heinz W. Engl and **Philipp Kügler** [1]

Oxford Centre for Industrial and Applied Mathematics
Mathematical Institute
University of Oxford
24-29 St Giles'
Oxford, OX1 3LB, UK

Abstract

Motivated by a parameter identification problem for a fourth-order partial differential equation which models the design of car windshields by the sagging process, we numerically study a parameter identification problem which is of second order as an equation for the parameter. The error magnitude and structure for a regularized Landweber method for solving this nonlinear inverse problem depend markedly on the type of this second order equation.

1 Motivation

Car windscreens are widely produced by using the gravity bending process: A sheet of glass is put onto a frame and heated from below. The glass gets viscous due to the temperature rise and sags under the force of gravity. The amount of bending depends on Young's modulus, which can be directly linked to the temperature. Thus, the aim to achieve a desired final shape can be seen as the inverse problem of determining Young's modulus (as a function of position) appropriately. Having determined Young's modulus can then be directly translated into an operating procedure of how to heat the glass sheet (see [6], [7] for details).

For a given Young's modulus $E = E(x,y)$, the displacement $w = w(x,y)$ of a glass sheet occupying a domain $\Omega \subset \mathbb{R}^2$ before the heating can be described approximately (see [7], [9]) by the (fourth order) linear elastic plate equation

$$\begin{aligned}(E(w_{xx}+\nu w_{yy}))_{xx} + 2(1-\nu)(Ew_{xy})_{xy} + (E(w_{yy}+\nu w_{xx}))_{yy} &= -\frac{12(1-\nu^2)}{h^3} f \text{ in } \Omega \\ w &= g \text{ on } \partial\Omega, \qquad (1.1)\end{aligned}$$

[1] on leave from: Institut für Industriemathematik, Johannes Kepler Universität, A–4040 Linz, Austria. E-Mail: engl@indmath.uni-linz.ac.at and kuegler@indmath.uni-linz.ac.at. Supported by the Austrian Fonds zur Förderung der wissenschaftlichen Forschung (projects F013-08 and P13478-INF), TMR (contract ERBFMRXCT 97-0117) and EPSRC grant GR/R06793/01

and an appropriate further boundary condition. Here, f is the gravity force, ν the Poisson ratio (assumed to be constant), g is a boundary value of w prescribed by a frame (lift-off, which is important in practice, is not considered here) and h is the thickness of the plate. In order to emphasize the dependence of the solution w of the *forward (*or *direct) problem* (1.1) on E, we denote it by $w = w(E)$.

Now assume that a "target" windscreen $\hat{w}$ is given. We want to find a Young's modulus $E = E(x, y)$ such that, if we put it into (1.1), the forward problem has $\hat{w}$ as its solution. We call this problem the *inverse problem*, although it could also be regarded as a control problem. In fact, for the industrial problem described, it is not important if E is uniquely determined, on the contrary, non-uniqueness gives more flexibility. However, viewing this problem as a inverse problem allows also to consider the "parameter identification problem" of determining E from distributed measurements of w, which is of independent interest.

If we assume $\hat{w}$ to be given, the inverse problem can be viewed as a second-order partial differential equation for E:

$$((\hat{w}_{xx} + \nu\hat{w}_{yy})E)_{xx} + 2(1-\nu)(\hat{w}_{xy}E)_{xy} + ((\hat{w}_{yy} + \nu\hat{w}_{xx})E)_{yy} = -\frac{12(1-\nu^2)}{h^3}f \quad \text{in } \Omega \tag{1.2}$$

The type of (1.2) depends on the sign of

$$\Delta = (\hat{w}_{xx} + \nu\hat{w}_{yy}) \cdot (\hat{w}_{yy} + \nu\hat{w}_{xx}) - 4(1-\nu)^2 w_{xy}^2 :$$

equation (1.2) is elliptic where $\Delta > 0$ and hyperbolic where $\Delta < 0$. Thus, the second order equation (1.2) for E would naturally call for boundary conditions for E on $\partial\Omega$ in the purely elliptic case ($\Delta > 0$ on Ω) and for Cauchy data on a suitable (non-characteristic) part $\Gamma \subset \partial\Omega$ in the purely hyperbolic case ($\Delta < 0$ on Ω). This is at least important if we consider the parameter identification problem, where uniqueness is desired. But also for the control problem, it is of interest which side conditions may (or should) be prescribed for E. Usually, parameter identification problems are, when viewed as equations for the parameter, of first order: e.g., the probably most widely studied parameter identification problem is that of identifying $q = q(x, y)$ in $-\nabla \cdot (q\nabla u) = f$ (with boundary conditions on u) from measurements of u. Our inverse problem (1.2) is, however, of second order in E. It is the purpose of this paper to study (mostly numerically) which consequences this has.

In the windshield design problem, the prescribed shape $\hat{w}$ is frequently such that Δ changes sign in Ω, so that (1.2) is an equation of mixed type in E. It would be of interest to give conditions which ensure solvability of (1.2), i.e., attainability of $\hat{w}$ by an appropriate Young's modulus E, which, for physical and technical reasons, also will have to fulfill constraints. We (have to) postpone this question for future work, but study the mixed problem numerically. We will see that the type of (a simplified version of) (1.2) has considerable influence on the error level and error structure of an iterative algorithm for solving the inverse problem.

Parameter identification problems are usually not tackled by numerically solving the pde-formulation (in our case (1.2)), but via an "output-least-squares" formulation, where the functional

$$E \to \|w(E) - \hat{w}\|^2 \tag{1.3}$$

is minimized over a feasible set for E. This is more appropriate for both the inverse and the control problem, since it allows the incorporation of noise (or a desired accuracy) in $\hat{w}$. Of course, the choice of the norm in which noise or accuracy are measured is important. For the windshield design problem, this norm should certainly involve curvature terms.

In this paper, we study a simplified problem, which shares with the motivating windshield problem the following two features:

1. The partial differential equation for the parameter E is of second order.
2. The type of this equation can be purely elliptic, hyperbolic or mixed, depending on the given target $\hat{w}$.

The simplification lies in the fact that our equation should also be of second order in w.

With the Tricomi equation

$$x\frac{\partial^2 u}{\partial x^2} + \frac{\partial^2 u}{\partial y^2} = f$$

- the probably most widely studied equation of mixed type - in mind, we have chosen the following equation as our *direct problem*:

Given a parameter E, find the solution $w = w(E)$ of

$$\begin{aligned} -\nabla \cdot (E\nabla w) - \nabla \cdot \left(\begin{pmatrix} w & 0 \\ 0 & 1 \end{pmatrix} \nabla E \right) &= f \text{ in } \Omega & (1.4) \\ w &= g \text{ on } \partial\Omega. & (1.5) \end{aligned}$$

The corresponding *inverse problem* is to find a parameter E such that $w(E) = \hat{w}$ (in the sense of minimizing (1.3)) for a given target $\hat{w}$ satisfying $\hat{w} = g$ on $\partial\Omega$. Formulated as an equation in E, this amounts to solving

$$-(\hat{w}E_x)_x - E_{yy} - (\hat{w}_x E)_x - (\hat{w}_y E)_y = f \text{ in } \Omega. \tag{1.6}$$

The principal part of (1.6) is $-\hat{w}E_{xx} - E_{yy}$ and hence, the equation is

- elliptic for $\hat{w} > 0$
- hyperbolic for $\hat{w} < 0$.

For $\hat{w}(x, y) = x$, (1.6) relates to the Tricomi equation of mixed type if $\hat{w}$ changes sign in Ω.

In Section 2, we briefly discuss the solvability of the direct problem (1.4), (1.5) in the sense of weak solutions $w(E)$ in $H^1(\Omega)$ for E out of a set K of admissible parameters. Section 3 focuses on the inverse problem in more detail. We first investigate the second order equation for the parameter E with respect to the question of appropriate conditions for E on the boundary. Then we describe the output-least-squares approach taken to solve the inverse problem numerically, where we take advantage of the adjoint method in order to reduce the numerical effort of our minimization routine. As to be expected for an inverse problem, ill-posedness is observed: small perturbations of the "data" $\hat{w}$ can lead to large changes in E. Thus, we construct an iterative regularization algorithm to solve the inverse problem in a stable way.

The new feature of this paper is an analysis of the behaviour of this regularization algorithm in dependence of the type of the equation (1.6). It turns out that, although this equation is not solved directly, its type also strongly influences the results obtained by the output-least-squares method: Our numerical results obtained for the parameter E in the hyperbolic case strongly differ from the elliptic case. Going from the purely hyperbolic case via mixed type to the purely elliptic case for (1.6), we come to the conclusion: "the more elliptic, the better the result". Note that we use prescribed boundary values for E, which is appropriate if (1.6) is elliptic, but not for the hyperbolic case.

We briefly touch the question of using different side conditions for E. The point we want to make is that also for the behaviour of the output-least-squares approach, the type of the equation for the unknown parameter E matters if this parameter appears with second derivatives in the partial differential equation from whose solution it is to be identified.

2 The Direct Problem

Let Ω be an open, bounded, connected domain in $\mathbb{R}^2$ with piecewise smooth boundary $\partial\Omega$. Our (simplified) direct problem consists in solving the second order equation for w

$$\begin{aligned} -\nabla \cdot (E \nabla w) - \nabla \cdot \left(\begin{pmatrix} w & 0 \\ 0 & 1 \end{pmatrix} \nabla E \right) &= f \text{ in } \Omega && (2.1) \\ w &= g \text{ on } \partial\Omega && (2.2) \end{aligned}$$

for a given parameter E, i.e.,

$$-(E w_x)_x - (E w_y)_y - w_x E_x - E_{xx} w = f + E_{yy}. \qquad (2.3)$$

If E is strictly positive in Ω, (2.3) is elliptic. We furthermore assume that

$$E, E_x, E_{xx} \in L^\infty(\Omega),$$

and - as E_{yy} is to be seen as part of the right-hand side in (2.3) - that

$$E_{yy} \in L^2(\Omega).$$

For brevity, we now define a linear operator L by

$$Lw := -(Ew_x)_x - (Ew_y)_y - E_x w_x - E_{xx} w$$

and set

$$\tilde{f} := f + E_{yy}.$$

Because of the linearity it then suffices to consider the boundary value problem with homogeneous Dirichlet condition

$$\begin{aligned} Lw &= \tilde{f} \text{ in } \Omega \qquad (2.4)\\ w &= 0 \text{ on } \partial\Omega, \qquad (2.5) \end{aligned}$$

since, if g is sufficiently smooth, a solution of (2.1), (2.2) can be constructed from one of(2.4), (2.5) using the Trace Theorem. According to the Lax-Milgram Lemma and the Fredholm Alternative (see [5]), precisely one of the following two statements holds:

1. either, for each $\tilde{f} \in L^2(\Omega)$ there exists a unique weak solution $w \in H_0^1(\Omega)$ of the boundary value problem (2.4), (2.5),

2. or else, there exists a weak solution $w \neq 0$ of the homogeneous problem

$$\begin{aligned} Lw &= 0 \text{ in } \Omega \qquad (2.6)\\ w &= 0 \text{ on } \partial\Omega. \qquad (2.7) \end{aligned}$$

Furthermore, should the second assertion hold, the dimension of the subspace $N \subset H_0^1(\Omega)$ of weak solutions of (2.6), (2.7) is finite and equals the dimension of the subspace $N^* \subset H_0^1(\Omega)$ of weak solutions of

$$\begin{aligned} L^* v &= 0 \text{ in } \Omega\\ v &= 0 \text{ on } \partial\Omega, \end{aligned}$$

where L^* is the (H^1-) adjoint operator to L. Finally, the boundary value problem (2.4), (2.5) has a weak solution if and only if

$$\int_\Omega \tilde{f} v d\vec{x} = 0 \text{ for all } v \in N^*.$$

We give a sufficient condition for $\dim N = \dim N^* = 0$, i.e., for the unique solvability of (2.4), (2.5), and hence of (2.1), (2.2). If we define the linear operator $\tilde{L}$ as

$$\tilde{L}w := Lw + E_{xx}w,$$

then, the boundary value problem (2.6), (2.7) becomes

$$\begin{aligned} \tilde{L}w - E_{xx}w &= 0 \text{ in } \Omega &(2.8)\\ w &= 0 \text{ on } \partial\Omega. &(2.9) \end{aligned}$$

Under the assumption that

$$E_{xx} \leq 0 \text{ in } \Omega, \tag{2.10}$$

the weak maximum principle (see [5]) implies that (2.8), (2.9) admits only the trivial solution, hence $\dim N = 0$. Note that (2.10) is sufficient but not necessary for uniqueness: e.g., if E_{xx} is a positive constant not contained in the spectrum of $\tilde{L}$, uniqueness holds. This is also the case if $\lambda = 1$ is no eigenvalue of the generalized eigenvalue problem

$$\tilde{L}w - \lambda E_{xx}w = 0$$

(see (2.8)). For the inverse problem, we choose

$$K = \left\{E \in H^1(\Omega) \mid E \geq \alpha > 0, E, E_x, E_{xx} \in L^\infty(\Omega) \text{ and } E_{yy} \in L^2(\Omega)\right\}, \tag{2.11}$$

(where α is a positive constant) as admissible set.

3 The Inverse Problem

For the inverse of determining the parameter E from data $\hat{w}$, we consider the output-least-squares formulation of minimizing the functional (1.3). There is a wide range of regularization methods for solving this ill-posed problem (see [2], [1]). We assume that we are given noisy data $\hat{w}^\delta$ with the information that

$$\|\hat{w} - \hat{w}^\delta\| \leq \delta, \tag{3.1}$$

where δ is the noise level. For the control problem, where $\hat{w}$ is not measured but prescribed, δ can be seen as the desired accuracy for the resulting w. Due to the ill-posedness, a mere minimization of the functional (1.3) leads to unstable results and to an error behaviour as shown in Figures 3.0.2 and 3.0.1 (taken from Section 4): while the error in the output, i.e., $\|w(E_k) - \hat{w}^\delta\|$ drops with the iteration index k of an iterative method, the error in the parameter, i.e., $\|E_k - E\|$, increases with ongoing iteration due to noise propagation. In order to provide a stable approximation of the true parameter E, the

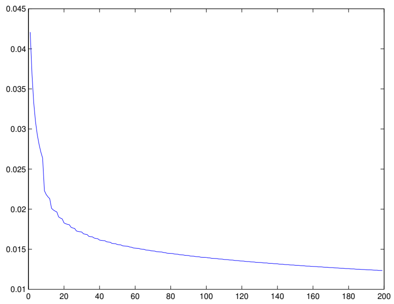

Figure 3.0.1: error in the output vs. k

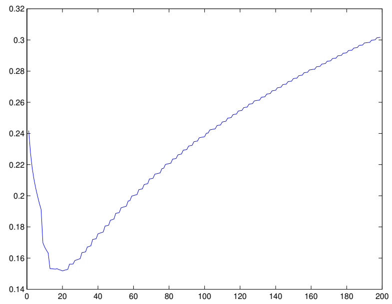

Figure 3.0.2: error in the parameter vs. k

iteration has to be stopped at the right place. An example for such a "stopping rule", is the "discrepancy principle" (see [2]) where the iteration is stopped at the index k^* with

$$\|\hat{w}^\delta - w(E_{k^*})\| \le \tau\delta < \|\hat{w}^\delta - w(E_k)\|, \quad 0 \le k \le k^*, \tag{3.2}$$

where the parameter τ is in the order of magnitude 2 (depending on properties of the linearized direct problem). See [4] for a survey on iterative regularization methods for nonlinear inverse problems, where questions like stability, convergence and rate of convergence of such methods are discussed.

Before introducing a very basic iterative regularization method, we first consider our inverse problem by plugging the data $\hat{w}$ into the partial differential equation (2.3). As mentioned above, our inverse problem has the specific feature that also second derivatives of the unknown parameter appear, which is unusual. An equally unusual way to attack the inverse problem would be to solve the second order partial differential equation

$$-\hat{w}E_{xx} - E_{yy} - 2\hat{w}_x E_x - \hat{w}_y E_y - \Delta\hat{w}E = f \quad \text{in} \quad \Omega. \tag{3.3}$$

for E. This equation (3.3) is

- elliptic where $\hat{w} > 0$, and
- hyperbolic where $\hat{w} < 0$.

In the purely elliptic case, i.e., if $\hat{w} > 0$ in all of Ω, we would naturally impose boundary conditions on E. If we choose Dirchlet conditions

$$E = b \quad \text{on} \quad \partial\Omega, \tag{3.4}$$

we can argue similarly as in Section 2 and guarantee the existence of a unique weak solution $E \in H^1(\Omega)$ provided that $\Delta\hat{w}$ is no (generalized) eigenvalue of $\bar{L}$ defined by

$$\bar{L}E := -\hat{w}E_{xx} - E_{yy} - 2\hat{w}_x E_x - \hat{w}_y E_y.$$

In the purely hyperbolic case, one would naturally impose Cauchy data

$$E = b \text{ and } \frac{\partial E}{\partial n} \quad \text{on} \quad \Gamma, \tag{3.5}$$

where Γ is a non-characteristic part of the boundary $\partial\Omega$. This part Γ should be chosen such that characteristics of (3.3) just cover Ω, but do not intersect. But what kind of boundary conditions on E should be prescribed for a mixed type problem where $\hat{w}$ changes its sign within Ω ? In the formulation (3.3) for the inverse problem, these questions about side conditions for E arise naturally. This is not the case for the output-least-squares formulation. Nevertheless, we will see that also for this formulation, these considerations are of importance. We mention again that the output-least-squares formulation of the inverse problem is more appropriate because of its ability to include noise or a desired accuracy via (3.1).

We now describe the iterative method we chose for solving our inverse problem of minimizing (1.3) over the admissible set K as given in (2.11): We define an operator F mapping the parameter $E \in K$ onto the weak solution w of the elliptic forward problem (2.1), (2.2), i.e.,

$$\begin{aligned} F : D(F) \subset K &\rightarrow L^2(\Omega), \\ E &\rightarrow w(E). \end{aligned}$$

Section 2 gives sufficient conditions for E being in $D(F)$. Note that although (3.3) is linear, the operator F is nonlinear.

For the inverse problem, we use the Landweber iteration method defined via

$$E_k = E_{k-1} + \omega F'(E_{k-1})^*(\hat{w} - F(E_{k-1})), \tag{3.6}$$

where the linear operator $F'(\cdot)$ is the Fréchet-derivative of F and $F'(\cdot)^*$ is its adjoint operator (with respect to the chosen Hilbert space structures H^1 and L^2, respectively). Here, ω is a real relaxation parameter ensuring nonexpansivity of the iteration map (see [4]), which we choose by a line search algorithm. Though we use it for our numerical tests, also in order to accelerate the convergence, we put, for simplicity of notation only, $\omega = 1$ in our further discussions.

Note that (3.6) is equivalent to

$$(E_k, h)_H = (E_{k-1}, h)_H + (\hat{w} - F(E_{k-1}), F'(E_{k-1})h)_{L^2(\Omega)} \tag{3.7}$$

for all directions $h \in H$ with $H \subset H^1(\Omega)$ to be specified later. We now leave this abstract level and describe the iteration for our particular problem in detail:

Linearizing the direct problem (2.1), (2.2) with respect to the parameter E in a direction h, we obtain

$$
\begin{aligned}
-\nabla\cdot(E\nabla\tilde{w}) - \nabla\cdot\left(\begin{pmatrix}\tilde{w} & 0\\ 0 & 0\end{pmatrix}\nabla E\right) &= \nabla\cdot(h\nabla w) + \nabla\cdot\left(\begin{pmatrix}w & 0\\ 0 & 1\end{pmatrix}\nabla h\right) \quad (3.8)\\
&\quad \text{in } \Omega\\
\tilde{w} &= 0 \text{ on } \partial\Omega, \quad (3.9)
\end{aligned}
$$

where w is the solution of (2.1), (2.2). Hence, the Fréchet-derivative of F at a point E is formally defined as

$$F'(E) : h \to \tilde{w},$$

where $\tilde{w}$ is the solution of the linearized problem (3.8), (3.9). Now, (3.7) requires to compute

$$(\hat{w} - F(E), F'(E)h)_{L^2(\Omega)} \tag{3.10}$$

in each step k for all directions h. In case of a n-dimensional parameter space this would mean that we have to solve the linear equation (3.8) n times per iteration step. In order to reduce the numerical effort we take advantage of an adjoint problem: If u is the solution of

$$
\begin{aligned}
-\nabla\cdot(E\nabla u) - \nabla\cdot\left(\begin{pmatrix}u & 0\\ 0 & 0\end{pmatrix}\nabla E\right) &= w - \hat{w} \text{ in } \Omega \quad (3.11)\\
u &= 0 \text{ on } \partial\Omega, \quad (3.12)
\end{aligned}
$$

where w is the solution of (2.1), (2.2), one gets via integration by parts that

$$(\hat{w} - F(E), F'(E)h)_{L^2(\Omega)} = -\int_\Omega h\nabla w\cdot\nabla u d\vec{x} - \int_\Omega w h_x u_x d\vec{x} - \int_\Omega h_y u_y d\vec{x} \tag{3.13}$$

holds. Hence, we only have to solve the "adjoint problem" (3.11), (3.12) and then use (3.13) to compute (3.10). Hence, if we use an n-dimensional parameter space in our computations, it is in each iteration step only necessary to solve equation (3.11), (3.12) once before building the scalar product in the right-hand side of (3.13) with n basis vectors $h_1, ..., h_n$. In this way, the iteration can be carried out efficiently.

Returning to (3.7), setting $\bar{E}_k = E_k - E_{k-1}$, $w_{k-1} = F(E_{k-1})$, and denoting the solution of (3.11), (3.12), at the iteration step $(k-1)$, by u_{k-1}, we get with (3.13)

$$(\bar{E}_k, h)_H = -\int_\Omega h\nabla w_{k-1}\cdot\nabla u_{k-1} d\vec{x} - \int_\Omega \left(\begin{pmatrix}w_{k-1} & 0\\ 0 & 1\end{pmatrix}\nabla u_{k-1}\right)\cdot\nabla h d\vec{x} \tag{3.14}$$

Equation (3.14) now can be interpreted as the weak formulation of either the equation

$$
\begin{aligned}
\bar{E}_k - \Delta \bar{E}_k &= -\nabla u_{k-1} \cdot \nabla w_{k-1} + \nabla \cdot \left(\begin{pmatrix} w_{k-1} & 0 \\ 0 & 1 \end{pmatrix} \nabla u_{k-1} \right) \text{ in } \Omega & (3.15) \\
\frac{\partial \bar{E}_k}{\partial n} &= \left(\begin{pmatrix} w_{k-1} & 0 \\ 0 & 1 \end{pmatrix} \nabla u_{k-1} \right) \cdot \vec{n} \text{ on } \partial\Omega & (3.16)
\end{aligned}
$$

for the choice $H = H^1(\Omega)$, or the equation

$$
\begin{aligned}
\bar{E}_k - \Delta \bar{E}_k &= -\nabla u_{k-1} \cdot \nabla w_{k-1} + \nabla \cdot \left(\begin{pmatrix} w_{k-1} & 0 \\ 0 & 1 \end{pmatrix} \nabla u_{k-1} \right) \text{ in } \Omega & (3.17) \\
\bar{E}_k &= 0 \text{ on } \partial\Omega & (3.18)
\end{aligned}
$$

for the choice $H = H_0^1(\Omega)$.

We summarize the way we perform Landweber iteration for our inverse problem:

1. Given E_{k-1}, calculate the solution w_{k-1} of the forward problem (2.1), (2.2).
2. Build the residual $w_{k-1} - \hat{w}$ and compute the solution u_{k-1} of the adjoint problem (3.11), (3.12).
3. Depending on the choice of H, solve equation (3.15), (3.16) or (3.17), (3.18) for the update $\bar{E}_k$, respectively.
4. $E_k = E_{k-1} + \bar{E}_k$.

The choice of the space H, i.e., between (3.15) or (3.17) is crucial with respect to our considerations above concerning side conditions: Since (3.16) depends on the iteration index $(k-1)$ and the adjoint solution u_{k-1}, which both do not appear in (3.3), condition (3.16) cannot be transformed into any boundary data on E for the second order equation (3.3). On the other hand, condition (3.18) is to be used if we want to prescribe Dirichlet boundary conditions in (3.3) on E. If E_{k-1} satisfies (3.4), and the update $\bar{E}_k$ vanishes on $\partial\Omega$ by (3.18), then also E_k fulfils (3.4). In all our numerical experiments, we used (3.17), (3.18), i.e., (3.14) with $H = H_0^1(\Omega)$, which means that we prescribe Dirichlet boundary conditions on E. The initial guess for the iteration then had to be chosen as to fulfill these boundary conditions.

4 Numerical Experiments

We present numerical examples for the inverse problem in the following form:
Given some target $\hat{w}$ being strictly positive, negative or alternating in sign and some prescribed boundary values b, find the minimizer of

$$
E \to \|\hat{w} - w(E)\|^2_{L^2(\Omega)} \tag{4.19}
$$

over K with $E|_{\partial\Omega} = b$, where $w(E)$ is the solution of (2.1), (2.2). We use the L^2-norm in (4.19) for simplicity, although for the inverse windshield problem motivating this work, a norm incorporating the curvature of $w(E)$ would be more appropriate. Our goal is to answer the following question (by numerical evidence):

(Q) Does a change of type in the equation (3.3) for the parameter E influence the result of the output-least-squares method, though we actually never solve this equation in our computations ?

In our first example we compare a purely elliptic with a purely hyperbolic problem. By the terms “elliptic”, “hyperbolic” and “mixed”, we always refer to (3.3) as an equation for E.

4.1 The Elliptic vs. the Hyperbolic Case

Let Ω be the unit circle. Then, for a parameter E as in Figure 4.1.1 and right hand sides

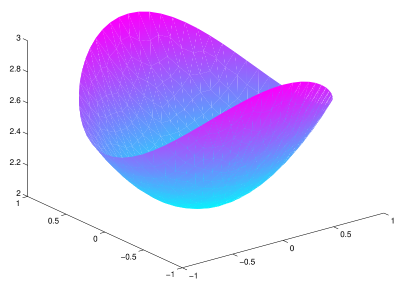

Figure 4.1.1: $E = 2 + \frac{1}{2}x^2 + y^2$

f as in Figures 4.1.2 and 4.1.3, the solutions $w(E)$ of the direct problem (2.1), (2.2) with

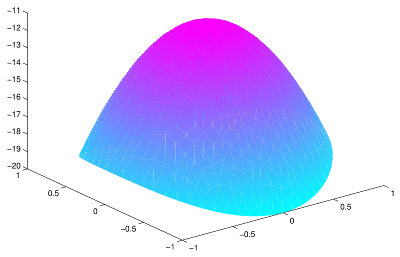

Figure 4.1.2: $f = -11 - 7x^2 - 9y^2$

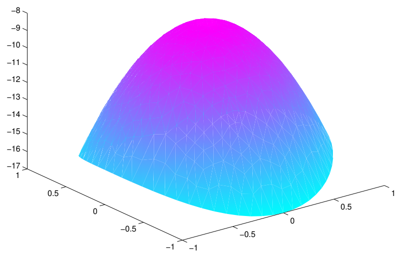

Figure 4.1.3: $f = -8 - 7x^2 - 9y^2$

$g = 2$ and $g = -1$, respectively, are shown in Figures 4.1.4 and 4.1.5. For the inverse

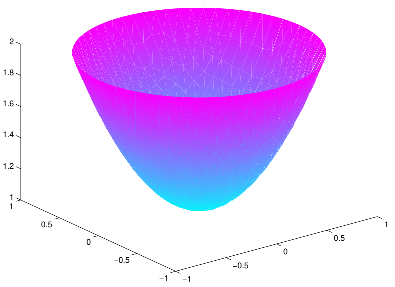

Figure 4.1.4: $w(E) = 1 + x^2 + y^2$

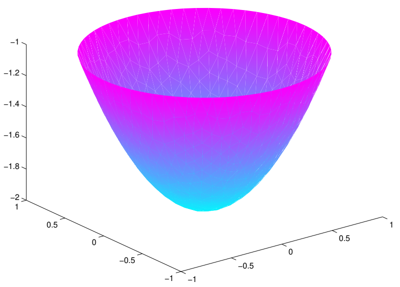

Figure 4.1.5: $w(E) = -2 + x^2 + y^2$

problem, we now consider Figures 4.1.4 and 4.1.5 as our data. Then, we clearly are in a purely elliptic situation, as $\hat{w}$ is strictly positive, while Figures 4.1.5 and 4.1.3 represent a purely hyperbolic case. Note that the underlying direct problems for both cases are close to each other, only different by a constant in f and g.

Starting the Landweber iteration as discussed in Section 3 with a initial guess E_0 (see Figure 4.1.6) satisfying $E_0|_{\partial\Omega} = E|_{\partial\Omega}$, we get a error behaviour as documented in Fig-

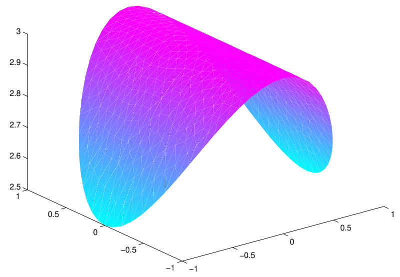

Figure 4.1.6: $E_0 = 3 - \frac{1}{2}x^2$

ures 4.1.7 and 4.1.8. While the relative error in the output $\frac{\|\hat{w} - w(E_k)\|_{L^2(\Omega)}}{\|\hat{w}\|_{L^2(\Omega)}}$ decreases in a similar way in the hyperbolic (green line) and the elliptic (red line) case, the parameter E is much better estimated in the elliptic case: After 200 iterations, the relative error in the parameter $\frac{\|E - E_k\|_{H^1(\Omega)}}{\|E\|_{H^1(\Omega)}}$ is about 5% in the elliptic case, but 10% in the hyperbolic case.

The really interesting observation, however, lies in the structure of the absolute error $E - E_k$ (see Figures 4.1.9 and 4.1.10, and in a bird's eye view, Figures 4.1.11 and 4.1.12): While in the elliptic case, rings seem to emanate from the boundary of the domain, the hyperbolic result still keeps some symmetry, but now not at all in a circular way. Rather a cross-shaped valley lies between the summits of the absolute error.

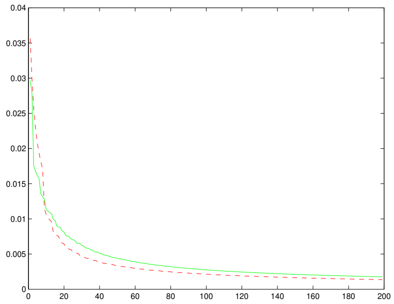

Figure 4.1.7: $\frac{\|\hat{w}-w(E_k)\|_{L^2(\Omega)}}{\|\hat{w}\|_{L^2(\Omega)}}$ vs. k

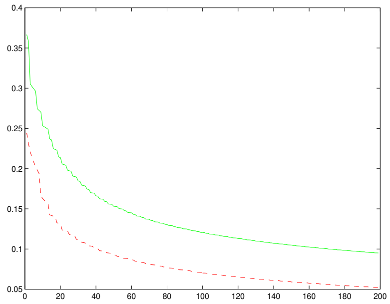

Figure 4.1.8: $\frac{\|E-E_k\|_{H^1(\Omega)}}{\|E\|_{H^1(\Omega)}}$ vs. k

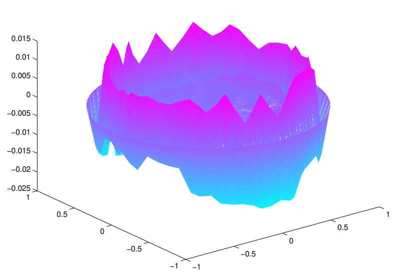

Figure 4.1.9: $E - E_{190}$, elliptic case

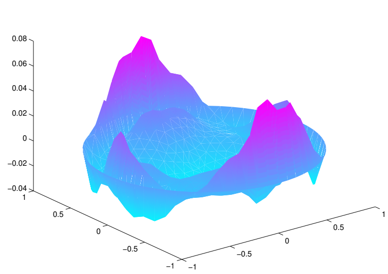

Figure 4.1.10: $E - E_{190}$, hyperbolic case

Before investigating the markedly different error structure more closely in Section 4.2, we briefly report on the effect of noise in the data $\hat{w}$. Using noisy data $\hat{w}^\delta$ with an L^2-norm error of approximately 2% instead of the data from Figures 4.1.4 and 4.1.5, the iteration shows the behaviour (sometimes called "semi-convergence") which is typical for ill-posed problems, see Figure 4.1.14: While the error in the output (Figure 4.1.13) decreases with k, the error in the parameter increases after a certain number of iterations. Now, even in the quality of the computed output a slight discrepancy between the elliptic (red line) and the hyperbolic (green line) case is noticeable, whereas it is much more evident in the estimation of E itself: The green line lies markedly above the red line, which had to be expected from the results about the noise-free case above. However, the instability comes in at roughly the same iteration index, i.e., the elliptic and hyperbolic cases seem to differ only in the achievable accuracy for noise-free data, not in the noise sensitivity.

In order to guarantee a stable approximation of E, the iteration has to be stopped in time. Applying the discrepancy principle (3.2) with $\tau = 1$ leads to a stop after only 16

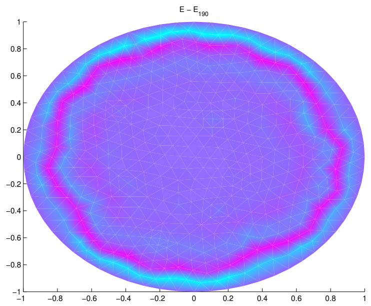

Figure 4.1.11: $E - E_{190}$, elliptic case, top view

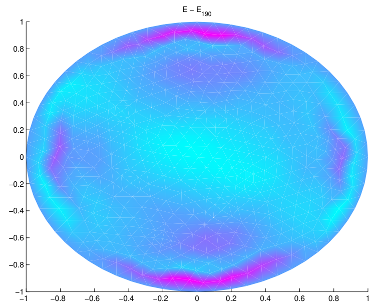

Figure 4.1.12: $E - E_{190}$, hyperbolic case, top view

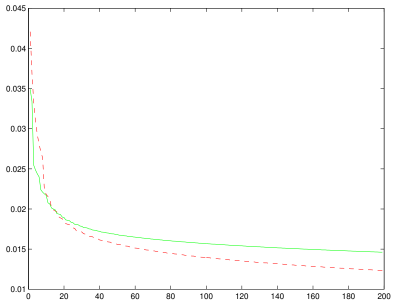

Figure 4.1.13: $\frac{\|\hat{w}^\delta - w(E_k)\|_{L^2(\Omega)}}{\|\hat{w}\|_{L^2(\Omega)}}$ vs. k

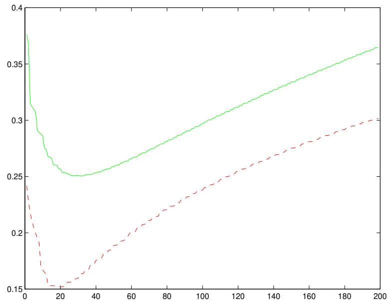

Figure 4.1.14: $\frac{\|E - E_k\|_{H^1(\Omega)}}{\|E\|_{H^1(\Omega)}}$ vs. k

iterations both in the elliptic and in the hyperbolic case. Note that even then, the relative error caused by 2% data noise is 15% in the elliptic case and even 25% in the hyperbolic one. This shows the ill-posed character of the problem.

4.2 The Mixed Case

We return to the situation of exact data and concentrate again on the error structure. As one could object to the comparison in Section 4.1 on the grounds that - though similar - the underlying direct problems are not exactly the same, we now consider a single mixed type problem. On the unit circle we choose

- again the true parameter E from Figure 4.1.1, and
- a right hand side $f = -2 - 3x$, being compatible with
- the data $\hat{w} = x$.

Now, the equation (3.3) obeyed by E is elliptic to the right and hyperbolic to the left of the origin, its principal part is that of the Tricomi equation. Starting again with E_0

from Figure 4.1.6, the absolute error $E - E_k$ after 190 iteration steps viewed from the top is shown in Figure 4.2.1. Again, the error in the elliptic region behaves completely

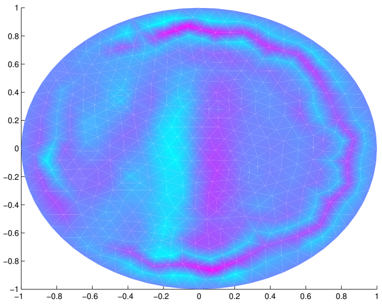

Figure 4.2.1: $E - E_{190}$, mixed case, top view

differently from the one in the hyperbolic part: Rings emanate from the right boundary but vanish when they reach the hyperbolic region. Furthermore, the border between both regions is clearly accented by a change of sign in $E - E_{190}$. This again clearly indicates that the type of (3.3) has direct consequences for the output-least-squares formulation of the inverse problem.

Now, for this mixed problem, we change E or $\hat{w}$, respectively. First, we keep $\hat{w}$ fixed and rotate E by 45 degrees counter-clockwise, resulting in

- $\hat{w} = x$
- $E = 2 + \frac{1}{2}\left(\sin(\frac{\pi}{4})x + \cos(\frac{\pi}{4})y\right)^2 + \left(\sin(\frac{\pi}{4})x - \cos(\frac{\pi}{4})y\right)^2$
- $f = -\frac{3}{2} - \frac{9}{2}x + y.$

For the second test, we keep E fixed and rotate $\hat{w}$, leading to

- $\hat{w} = \sin(\frac{\pi}{4})x + \cos(\frac{\pi}{4})y$
- $E = 2 + \frac{1}{2}x^2 + y^2$
- $f = -2 - 3\sqrt{\frac{1}{2}}x - 3\sqrt{\frac{1}{2}}y.$

Starting in both cases with an initial guess

- $E_0 = E + 1 - x^2 - y^2,$

the iteration yields absolute errors in the parameter as recorded in Figures 4.2.2 and 4.2.3, respectively. These results clearly indicate that the error structure observed is neither due to the parameter E to be identified nor to the right hand side f in the direct problem.

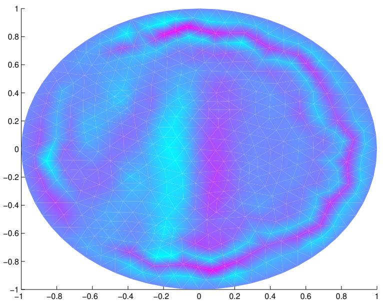

Figure 4.2.2: $E - E_{190}$ for $\hat{w} = x$

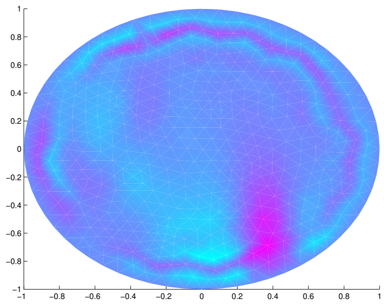

Figure 4.2.3: $E - E_{190}$ for $\hat{w} = \sin(\frac{\pi}{4})x + \cos(\frac{\pi}{4})y$

It is only the given data $\hat{w}$, which determines the elliptic and hyperbolic regions, that influences the outcome. While figure 4.2.2 is nearly identical to Figure 4.2.1 - though E has changed -, the structure in Figure 4.2.3 is different due to the rotation of $\hat{w}$. Although the error seems to follow the 45 degrees turn, it is noticeable that in this case the border between the hyperbolic and the elliptic regions is not that pronounced as in its counterpart to the left.

So, error structures are markedly different in elliptic and in hyperbolic regions, but why? A first idea towards a better understanding of the error behaviour is to look at the characteristics of equation (3.3) for the parameter E. Following [8], we compute the two characteristic directions for (3.3) by

$$\frac{dy}{dx} = \pm \frac{\sqrt{-\hat{w}}}{\hat{w}}. \tag{4.1}$$

Note that neither E nor f appear in (4.1), the characteristics only depend on the given data $\hat{w}$. They are only real and distinct in hyperbolic regions, i.e., where $\hat{w} < 0$. There, the characteristics are given by

$$\begin{aligned} y_1 &= c_1 + 2\sqrt{-x} \\ y_2 &= c_2 - 2\sqrt{-x} \end{aligned}$$

for constants c_1, c_2, some of them are plotted in Figure 4.2.4. Though both the error structure (see Figure 4.2.1) and the characteristics (Figure 4.2.4) only depend on $\hat{w}$, a direct connection between both pictures cannot be seen immediately.

4.3 A Sequence of Mixed Problems

Next, we consider a sequence of mixed problems where the elliptic region wanders from the boundary of the unit circle towards the center. Choosing

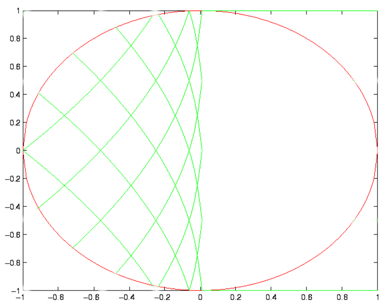

Figure 4.2.4: some characteristics for $\hat{w} = x$

- the parameter E from Figure 4.1.1
- and a fixed right hand side $f = -8$,

we created a sequence (Figures 4.3.1 - 4.3.4) of data by simply changing the boundary values for the direct problem:

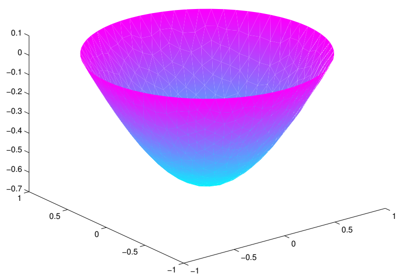

Figure 4.3.1: $w(E)$ with $w|_{\partial\Omega} = 0.05$

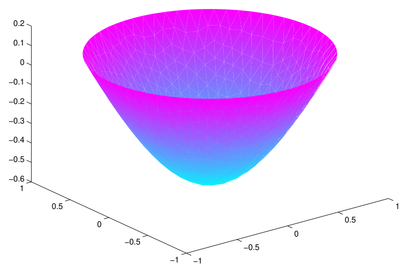

Figure 4.3.2: $w(E)$ with $w|_{\partial\Omega} = 0.1$

The “bowl” $\hat{w}$ is pulled out of the negative area, resulting in a growth of the elliptic region, coloured in red in Figures 4.3.5 - 4.3.8.

Starting again with E_0 from Figure 4.1.6, the iteration shows (see Figures 4.3.9 and 4.3.10) that the result gets better the “more elliptic” the problem gets. In the absolute error (see Figures 4.3.11 - 4.3.14), the peaks to the left and to the right smear out towards the center with the propagation of the ellipticity. Nevertheless, different from Example 4.2.1 in Section 4.3, no clear distinction between the elliptic and the hyperbolic region can be extracted from the error structure.

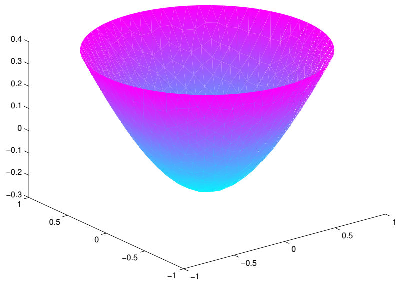

Figure 4.3.3: $w(E)$ with $w|_{\partial\Omega} = 0.4$

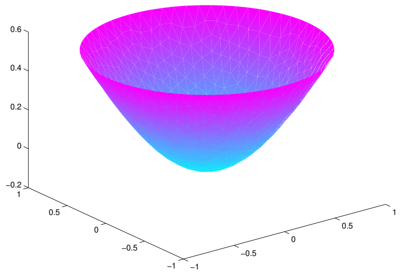

Figure 4.3.4: $w(E)$ with $w|_{\partial\Omega} = 0.55$

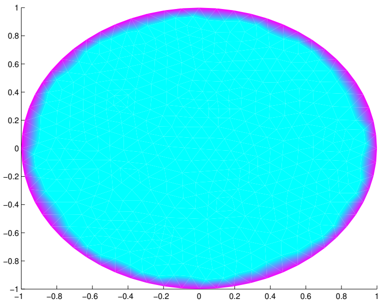

Figure 4.3.5: regions for $\hat{w}|_{\partial\Omega} = 0.05$

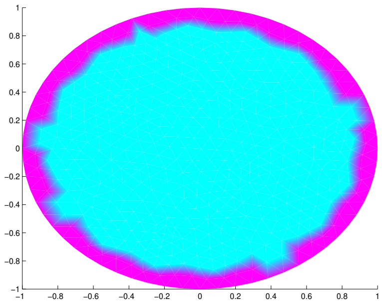

Figure 4.3.6: regions for $\hat{w}|_{\partial\Omega} = 0.1$

4.4 Another Sequence with the Hyperbolic Region Outside

We now look at mixed problems where the elliptic region is surrounded by the hyperbolic one. Choosing

- the parameter E from Figure 4.1.1
- and a right hand side $f = 8$,

we created two data sets (Figures 4.4.1 and 4.4.2) by changing the boundary values for the direct problem. The elliptic region, again coloured in red, now emanates from the center of the unit circle (Figures 4.4.3 and 4.4.4). Figures 4.4.5 and 4.4.6 show that - as in the previous section - the result gets better the more elliptic the problem gets. In the absolute error (see Figures 4.4.7 and 4.4.8), a front following the border between ellipticity and hyperbolicity can be observed, finally (as the hyperbolic region gets smaller) leading to a closed circle next to the boundary, as in the elliptic case.

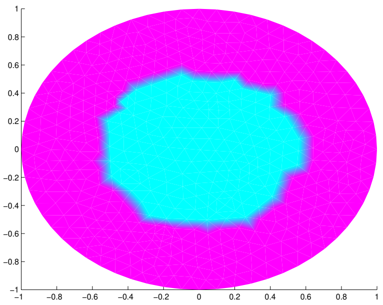

Figure 4.3.7: regions for $\hat{w}|_{\partial\Omega} = 0.4$

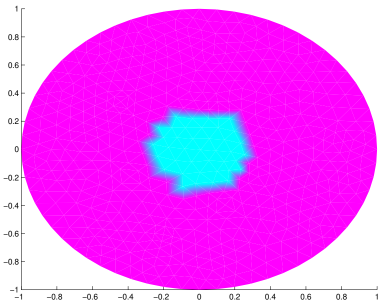

Figure 4.3.8: regions for $w|_{\partial\Omega} = 0.55$

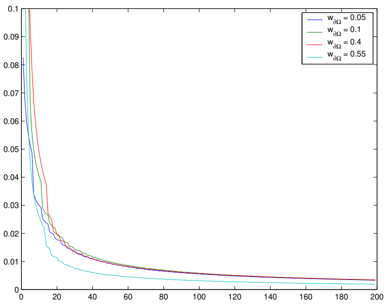

Figure 4.3.9: $\frac{\|\hat{w}-w(E_k)\|_{L^2(\Omega)}}{\|\hat{w}\|_{L^2(\Omega)}}$ vs. k

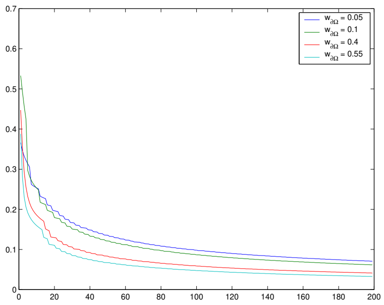

Figure 4.3.10: $\frac{\|E-E_k\|_{H^1(\Omega)}}{\|E\|_{H^1(\Omega)}}$ vs. k

4.5 Perturbation of the Parameter on the Boundary

We return to the discussions led in Sections 2 and 4.2. From the pde point of view, it would be natural to prescribe Cauchy data for E on $\partial\Omega$ (see (3.5)) in the purely hyperbolic situation ($\hat{w} < 0$). However, our implementation of Landweber iteration only allows to deal with Dirichlet conditions for E (see (3.4), (3.17) and (3.18)). Solving equation (3.3) for $\hat{w} < 0$ with a then unnatural boundary condition (3.4) is unstable. Having constructed a solution E by choosing $\hat{w}$ and f appropriately (as, e.g., in Section 4.1), already a small perturbation in the boundary data (3.4) causes trouble: in the hyperbolic case, the information propagates from the boundary along the characteristics into the interior of the domain. Now, as soon as the characteristics cross (as shown in Figure 4.5.1 for a single pair), the data - emanating from the four sections $\partial\Omega$ - for the crossing point are no longer compatible in case of perturbations on the boundary. As there are no real characteristics in the elliptic case ($\hat{w} > 0$), perturbations of the boundary data (3.4) do not have a dramatic impact on the solution.

Though we never really solve equation (3.3) in our output least squares approach, we still observe what is suggested by the pde theory. For the same setups as in Section 4.1

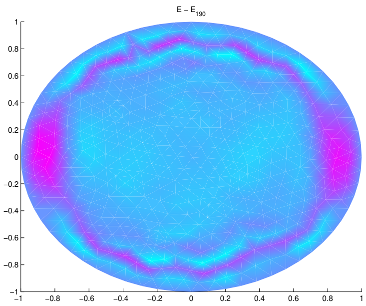

Figure 4.3.11: $E - E_{190}$, top view for $\hat{w}_{\partial\Omega} = 0.05$

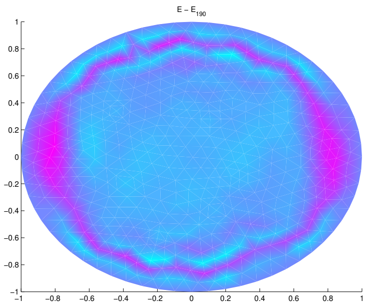

Figure 4.3.12: $E - E_{190}$, top view for $\hat{w}_{\partial\Omega} = 0.1$

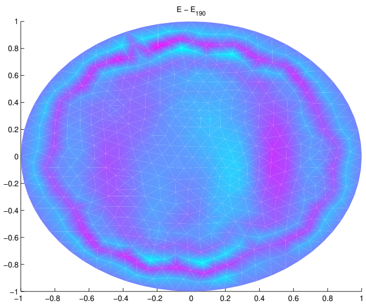

Figure 4.3.13: $E - E_{190}$, top view for $\hat{w}_{\partial\Omega} = 0.4$

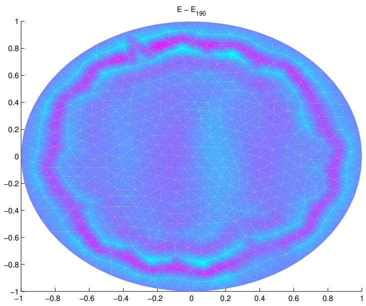

Figure 4.3.14: $E - E_{190}$, top view for $\hat{w}_{\partial\Omega} = 0.55$

and a starting parameter E_0 (see Figure 4.5.2) with slightly wrong boundary values, i.e. $E_0|_{\partial\Omega} \neq E|_{\partial\Omega}$, the results are shown in Figures 4.5.3 and 4.5.4. While in the elliptic case, the estimated parameter is close to the true one in spite of the wrong boundary values, in the hyperbolic case the deviation, especially in the center, is high.

We close this Section on numerical experiments by emphasizing that our results are not only valid for the unit circle. Tests which were done on an ellipse, a rectangle and the unit square, showed a similar behaviour as discussed above.

5 Conclusions and Outlook

Our numerical results clearly indicate that Landweber iteration for estimating the parameter E for the elliptic and hyperbolic cases of (3.3) behaves distinctively different, especially in the error structure of the estimated parameter. In the elliptic case, the shape of $\partial\Omega$ dominates the error pattern. All the elliptic examples show closed circular curves in the error in the neighbourhood of $\partial\Omega$. It is likely that this is due to the effect of

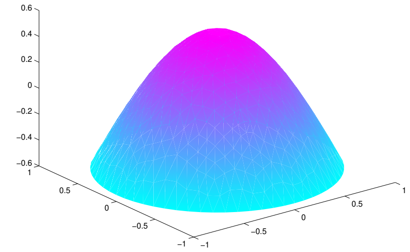

Figure 4.4.1: $w(E)$ with $w|_{\partial\Omega} = -0.55$

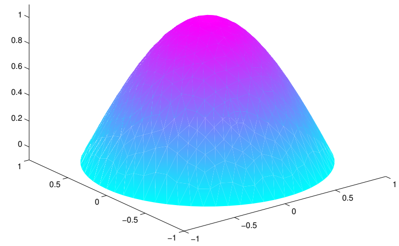

Figure 4.4.2: $w(E)$ with $w|_{\partial\Omega} = -0.05$

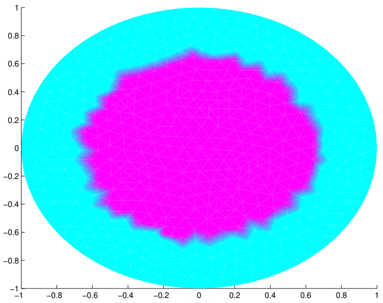

Figure 4.4.3: regions for $\hat{w}|_{\partial\Omega} = -0.55$

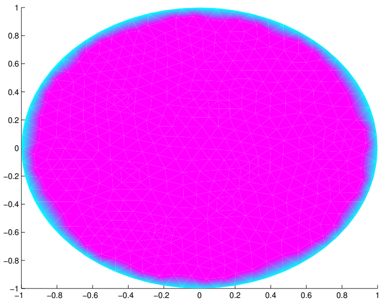

Figure 4.4.4: regions for $\hat{w}|_{\partial\Omega} = -0.05$

overshooting by the line search used in the iterative optimization routine. Nevertheless, the same algorithm was used for the hyperbolic case, and there these lines are interrupted, if appearing at all. In the hyperbolic case, the error pattern is mainly influenced by the given data $\hat{w}$ - which then determine two families of real characteristics -, and neither the parameter E itself nor the right hand side f in the direct problem have a noticeable effect.

The algorithm described in Section 3 performed well in matching the given data $\hat{w}$ by a computed output $w(E)$ both for elliptic and hyperbolic problems. However, the "true" parameter E could be determined much better in the elliptic case. As far as (in)stability is concerned, both cases show a similar behaviour. Having only considered prescribing Dirichlet boundary conditions on E, it is clear why the estimation of E is quite satisfactory in the elliptic case, for which (3.4) is natural, whereas for a hyperbolic problem, (3.4) is unnatural, which is reflected in a worse estimation result. Furthermore, a perturbation of the boundary data for E has a much stronger impact on the error in the hyperbolic case than in the elliptic one. It would be interesting to consider the case of prescribing Cauchy data. There, we expect the hyperbolic case to behave better, although that will depend on the part of the boundary where Cauchy data for E are prescribed. For the elliptic case,

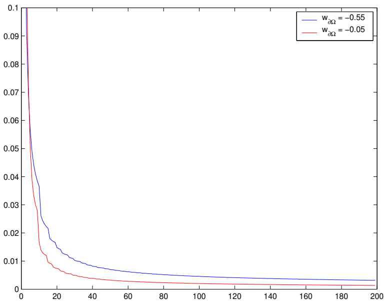

Figure 4.4.5: $\frac{\|\hat{w}-w(E_k)\|_{L^2(\Omega)}}{\|\hat{w}\|_{L^2(\Omega)}}$ vs. k

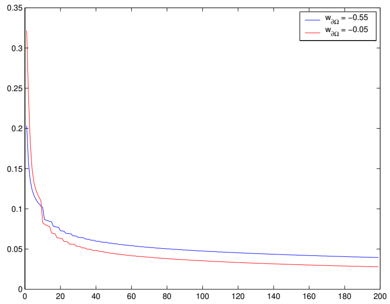

Figure 4.4.6: $\frac{\|E-E_k\|_{H^1(\Omega)}}{\|E\|_{H^1(\Omega)}}$ vs. k

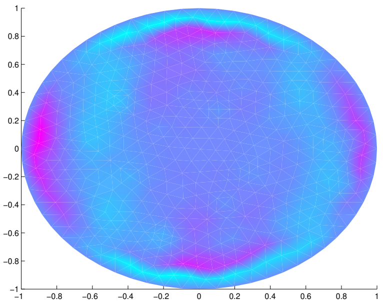

Figure 4.4.7: $E - E_{190}$, top view for $\hat{w}_{\partial\Omega} = -0.55$

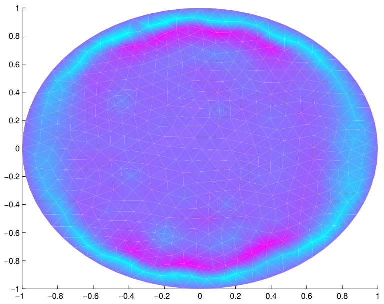

Figure 4.4.8: $E - E_{190}$, top view for $\hat{w}_{\partial\Omega} = -0.05$

the Cauchy problem is severely ill-posed (see, e.g., [3]), so that we have to expect severe difficulties. Usually, parameter estimation problems are considered to be mildly ill-posed. The argument just made shows that in cases where the parameter obeys a second order equation, the ill-posedness might become more severe due to the second derivatives. Our main point, however, is that in the case that the parameter appears in the direct problem with its second derivatives, the properties of the second order partial differential equation that the parameter fulfills also show up in the output-least-squares approach. This is also expected to have relevance for the windshield design problem, which motivated this study.

Acknowledgement: We thank D. Allwright, D. Gelder, J.R. Ockendon and D. Salazar-Gonzales for bringing the windshield problem to our attention, and for interesting discussions.

References

[1] T. Banks and K. Kunisch, Estimation Techniques for Distributed Parameter Systems, Birkhäuser, 1989

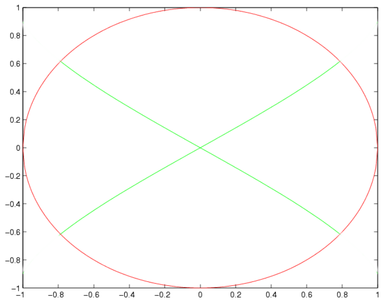

Figure 4.5.1: pair of characteristics for $\hat{w} = -2 + x^2 + y^2$

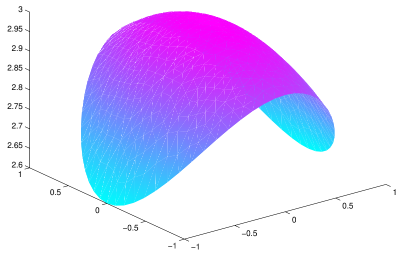

Figure 4.5.2: $E_0 = 3 - 0.4x.^2 - 0.1y.^2$

[2] H.W. Engl, M. Hanke and A. Neubauer, Regularization of Inverse Problems, Kluwer Academic Publishers, 1996 (Paperback edition 2000)

[3] H.W. Engl, A. Leitao, Convergence and regularizing properties of a Mann iterative method for elliptic Cauchy problems, submitted

[4] H.W. Engl, O. Scherzer, Convergence rates results for iterative methods for solving nonlinear ill-posed problems, in: D. Colton, H.W. Engl, A.K. Louis, J. McLaughlin, W.F. Rundell (eds.), Surveys on Solution Methods for Inverse Problems, Springer, Vienna/New York, 2000, pp. 7-34

[5] L.C. Evans, Partial Differential Equations, American Mathematical Society, 1998

[6] S. Manservisi, Control and optimization of the sag bending process in glass windscreen design, in: Leif Arkeryd, Jöran Bergh, Philip Brenner and Rolf Pettersson (eds.), Progress in Industrial Mathematics at ECMI 98, Teubner, Stuttgart 1999, pp. 97-105

[7] S. Manservisi, M. Gunzburger, A variational inequality formulation of an inverse elasticity problem, Applied Numerical Mathematics, 34 (2000), 99-126

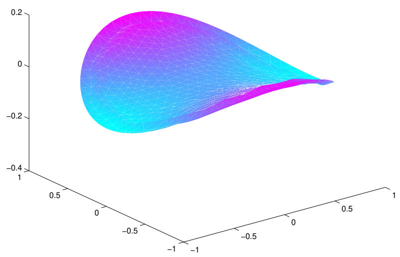

Figure 4.5.3: $E - E_{190}$, elliptic case

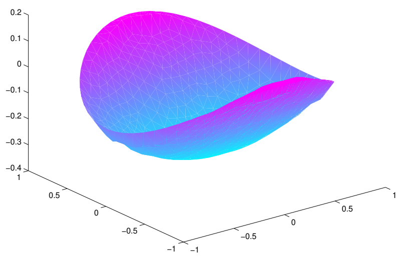

Figure 4.5.4: $E - E_{190}$, hyperbolic case

[8] J. Ockendon, S. Howison, A. Lacey and A. Movchan, Applied Partial Differential Equations, Oxford University Press, 1999

[9] S.P. Timoshenko, S. Woinowsky-Krieger, Theory of Plates and Shells, Mc Graw Hill Book Company, New York - Toronto - London, 1959